- 1 Classification: ocean acidification, end Cretaceous, Cretaceous-Paleogene extinction
- 2 event, K-Pg boundary, asteroid impact

3 Severity of ocean acidification following the end Cretaceous

4 asteroid impact

24

25

¹Corresponding author

5 Toby Tyrrell^{a,1}, Agostino Merico^{b,c}, David I. Armstrong M^cKay^a. 6 7 8 Correspondence to: Toby Tyrrell 9 Address: Ocean and Earth Science, National Oceanography Centre Southampton, University 10 of Southampton, Waterfront Campus, European Way, Southampton, SO14 3ZH 11 Telephone: +44 (0) 2380596110 12 E-mail: toby.tyrrell@noc.soton.ac.uk 13 14 15 16 ^a Ocean and Earth Science, National Oceanography Centre Southampton, University of 17 Southampton, Waterfront Campus, European Way, Southampton, SO14 3ZH, United 18 Kingdom 19 ^b Systems Ecology, Leibniz Center for Tropical Marine Ecology, Fahrenheitstraße 6, 28359 20 Bremen, Germany 21 ^c School of Engineering and Science, Jacobs University, Campus Ring 1, 28759 Bremen, 22 Germany 23

Most paleo-episodes of ocean acidification (OA) were either too slow or too small
to be instructive in predicting near-future impacts. The end-Cretaceous event (66
Mya) is intriguing in this regard, both because of its rapid onset and also because
many pelagic calcifying species (including 100% of ammonites and more than
90% of calcareous nannoplankton and foraminifera) went extinct at this time.
Here we evaluate whether extinction-level OA could feasibly have been produced
by the asteroid impact. Carbon cycle box models were used to estimate OA
consequences of: (A) vaporisation of up to 60×10^{15} moles of sulphur from
gypsum rocks at the point of impact; (B) generation of up to 5×10^{15} moles of
NOx by the impact pressure wave and other sources; (C) release of up to 6500 Pg
C from vaporisation of carbonate rocks, wildfires and soil carbon decay; and (D)
ocean overturn bringing high CO2 water to the surface. We find that the
acidification produced by most processes is too weak to explain calcifier
extinctions. Sulphuric acid additions could have made the surface ocean
extremely undersaturated ($\Omega_{calcite}$ less than 0.5), but only if they reached the
ocean very rapidly (over a few days) and if the quantity added was at top end of
literature estimates. We therefore conclude that severe ocean acidification might
have been, but most likely was not responsible for the great extinctions of
planktonic calcifiers and ammonites at the end of the Cretaceous.

46 Motivation

Significance

Ammonites went extinct at the time of the end-Cretaceous asteroid impact, as did more than 90% of species of calcium carbonate-shelled plankton (coccolithophores and foraminifera). Comparable groups not possessing calcium carbonate shells were less severely impacted, raising the possibility that ocean acidification, as a side-effect of the collision, might have been responsible for the apparent selectivity of the extinctions. We investigated whether ocean acidification could have caused the disappearance of the calcifying organisms. In a first detailed modelling study we simulated several possible mechanisms from impact to seawater acidification. Our results suggest that acidification was most probably not the cause of the extinctions.

47

48

Using Earth history to understand OA impacts.

49 From pre-industrial times up to the year 2008, ca. 530 Pg of carbon were added to the 50 atmosphere through burning of fossil fuels and deforestation (1). This has led to an 51 increase in atmospheric CO₂ of 40% (from 280 ppm in pre-industrial times to 400 52 ppm in the year 2015). Simultaneously, about 160 Pg C has been taken up by the 53 ocean (2), where it causes ocean acidification (hereafter 'OA') (3). 54 55 OA is of particular concern for calcifying organisms (3), because it leads to lower CO₃²- concentrations and hence lower seawater saturation states with respect to 56 57 $CaCO_3$ (Ω). In theory, lower Ω should make it energetically more costly for 58 organisms to synthesise CaCO₃ shells and skeletons and, subsequently, if Ω falls 59 below 1.0, to maintain them against dissolution. A large variety of short-term 60 experiments have been carried out to test for such consequences (4). It is widely 61 recognised, however, that one aspect which these experiments generally do not 62 address (although see refs. 5 and 6) is the degree to which organisms can evolve in 63 response to the changing carbonate chemistry and thereby become more tolerant of

the new conditions. As a result, there is a need for approaches that reveal the longterm response to OA with evolutionary adaptation factored in.

Events in the past could potentially shed more light on the evolutionary response to OA. However, a recent review (7) highlighted a major difficulty: during most suspected OA events, CO₂ levels rose so slowly that the carbonate compensation process, i.e. the automatic stabilising mechanism that opposes changes in ocean CaCO₃ saturation (8), must have interposed to alter the nature of the impacts (7,9,10), making them less useful for understanding the future.

In contrast, at the end of the Cretaceous the asteroid impact induced very sudden changes. Here we investigate the possibility that there was a sharp and sudden acidification event concentrated in surface waters (deep waters experience delayed and less severe acidification in response to an atmospheric source of acidity (11)). Because there are no paleo records with which to constrain seawater chemistry changes during the critical few years following the impact (the slow speed at which most ocean sediments accumulate limits the resolution of sediment records to thousands of years), we employ models to calculate how dramatic the surface OA may have been at the end Cretaceous.

Extinctions of calcifiers at the end of the Cretaceous.

Another reason for being particularly interested in the Cretaceous/Paleogene (K/Pg) boundary in the context of OA, is that many surface-dwelling calcifiers went extinct at this time (12). Ammonites had existed on Earth for some 300 million years, and had survived previous extinction events, including the one at the end of the Permian

when more than 95% of all marine species were lost, but they succumbed at the K/Pg (13). Within other groups of marine organisms there appears also to have been a strong extinction bias towards calcifiers. Among autotrophs, for example, more than 90% of all calcareous nannoplankton (coccolithophore) species went extinct at this time (14, 15). By contrast, there were much lower extinction rates for comparable non-calcareous groups, such as siliceous diatoms of which at most 50% of species went extinct (16, 17), organic-walled dinoflagellates which experienced no significant extinction (18), and non-calcifying haptophyte phytoplankton of which many clades survived the K/Pg (19). Similarly among heterotrophs, more than 95% of carbonate-shelled planktic foraminifera were lost (14) while only a few planktic silica-shelled radiolaria went extinct (16, 17). The particular severity of extinctions for calcifiers has led to suggestions (e.g. 20, 21) that they were caused by OA. However, as described later, upon a more detailed inspection of the paleontological evidence the selectivity of extinctions seems less clear-cut.

We used biogeochemical box models of the global carbon cycle (which simulate the organic and inorganic carbon pumps, ocean mixing, exchange of CO₂ between the ocean and atmosphere, and other processes) to assess whether severe OA might have occurred. Because of the absence of accompanying paleo data at this timescale, our aim is not to pin down the exact pattern of carbon chemistry changes that took place at the K/Pg. Instead we focus our attention on delineating the upper bound of OA severity. Our aim is to calculate the maximum degree of OA that might plausibly have occurred, not the most likely.

Comparison to previous studies of carbon chemistry at the K/Pg

A few other studies (21-25) have previously addressed carbon cycle and OA changes at the K/Pg. Beerling et al. (23) used data (the stomatal index of land plant leaves) and a box model; their data suggested that atmospheric pCO₂ increased from 350-500 ppmv to 2300 ppmv across the K/Pg boundary (although such a rise is not seen in other proxy data (24)), from which they inferred an instantaneous transfer of ca. 4,600 Pg C from rocks to the atmosphere.

D'Hondt et al. (25) used calculations rather than models to investigate the severity of surface OA at the K/Pg boundary. They calculated the consequences of acid creation (between 1×10^{16} and 1.3×10^{17} mol $H_2 SO_4$) from vaporisation of gypsum rocks at the site of impact, and, secondarily, from nitric acid. The lower amounts do not significantly affect surface ocean pH, according to their calculations, but the highest amounts would be large enough (>1.2 $\times 10^{17}$) to destroy entirely the carbonate buffer capacity of the upper 100 m of the modern global ocean and drive pH transiently to values as low as 3. However, such extreme pH changes are by no means necessary in order to make seawater strongly corrosive to CaCO₃ (Ω <1), which can be achieved by a pH drop of less than 1 unit from its modern value of just over 8.

We revisit the OA estimates of D'Hondt et al. (25), carrying out the first evaluation using an established dynamic ocean carbon cycle model (see Methods section and detailed methods in supplementary information). While D'Hondt et al. (25) focussed on how much acid is needed to overwhelm the entire buffering capacity of seawater, we focus instead on the consequences for Ω_{calcite} (the saturation state of seawater with respect to the calcite form of CaCO₃). We explicitly calculate and compare the

potential of different hypothesized sources of acidity to lower surface (0-100m) ocean pH and $\Omega_{calcite}$ at the end Cretaceous.

140

141

142

143

144

145

146

147

148

149

150

151

152

153

154

155

156

157

158

159

160

161

138

139

Results

(1) Sulphate aerosols due to impact on gypsum-rich rocks. An asteroid estimated at ~10km in diameter (26,27) hit the Earth at a point on the Yucatan peninsula in Mexico, producing the Chicxulub crater (diameter ~200 km). The target rocks (carbonate- and gypsum- or anhydrite-rich sediments underlain by granite crust) were partly ejected and partly volatilised by the impact. In addition to sulphur from the impact rocks, between 1 and 5 x 10¹⁵ Mol S could have come from the asteroid itself (28). Thermal decomposition of gypsum or anhydrite (we refer only to gypsum henceforth) is presumed (on the basis of laboratory volatilisation experiments; e.g. ref. 29) to have led to the near-instantaneous release of SO₃ (21) to the atmosphere according to the reaction: $CaSO_4 \rightarrow CaO + SO_3$ (1) According to this equation there is also a simultaneous equimolar production of base (in the form of lime, CaO), some of which could have counteracted the effects of the acid (30). However, consistent with our goal of estimating maximum possible impacts, lime effects are not included in any of the simulations in this study. Some of the SO₃ and CaO may have recombined within the plume back to solid CaSO4 (30,31).After being injected into the atmosphere, SO₃ would have been transformed to

sulphuric acid (H₂SO₄). There is some debate about how rapidly the H₂SO₄ arrived at

the ocean. Some understanding has been obtained from studies (32-34) of sulphur dynamics following volcanic eruptions such as Mount Pinatubo in 1991. Where S is injected into the stratosphere, its return to the Earth's surface is delayed, due in part to the lack of water vapour and rainfall there, typically taking a few years (34). Earlier modelling studies (35,31) suggested residence times of S in the atmosphere of several months to a few years. An alternative and very different scenario has recently been proposed for the K/Pg (21), in which sulphuric acid was transported much more rapidly to the ocean. It is suggested that, immediately after the impact, most of the sulphuric acid aerosols were scavenged by large silicate particles falling rapidly back to Earth, thereby delivering the H₂SO₄ to the ocean within only one or a few days.

D'Hondt et al. (25) estimated total sulphuric acid production to have been in the range 10 to 130 x 10¹⁵ mol H₂SO₄ (320 to 4160 Pg S), based on several earlier studies (36-38). Later studies suggested ~10-fold smaller total production of only 0.9 to 9 x 10¹⁵ mol H₂SO₄ (30 to 300 Pg S, ref. 31) and 2.4 to 11 x 10¹⁵ mol H₂SO₄ (78 to 364 Pg S, ref. 39). A recent review put the total sulphuric acid input at between 3 and 16 x 10¹⁵ mol or possibly higher (27).

We implemented this hypothesis in the model through a family of runs of different total sulphur addition (15, 30 and 60 x 10^{15} mol, corresponding to 480, 960 and 1920 Pg). We carried out a main set of runs using longer *e*-folding times of H₂SO₄ addition (0.5, 1, 5 and 10 years) and also additional runs with a shorter *e*-folding time of 10 hours, following ref. 21. H₂SO₄ addition reduces surface water total alkalinity (TA) in the molar ratio H₂SO₄:TA = 1:-2 (ref. 40).

Results of the main sulphuric acid addition runs are shown in the first (left-most) column in figure 1 (with sensitivity to rate of addition shown in Fig S1). The results of the additional runs with $\tau=10$ hours are shown in figure 2. There are very large impacts on pH and $\Omega_{calcite}$ for large sulphur inputs, which are exacerbated by rapid addition. The greatest effects are in the immediate aftermath and are of short duration (a few years).

<FIGURE 1 TO GO HERE>

(2) Carbon dioxide from carbonate rocks and organic carbon.

We consider all CO₂ sources together. In the same way that the impact released sulphur compounds from gypsum rocks as they were vaporised, vaporisation of carbonate rocks yielded CO₂. It has been estimated that an asteroid of diameter ~10 km hitting the 3 or 4 km thick layer of sedimentary carbonates of the Yucatan peninsula (27) would have released between about 5000 and 9000 Pg CO₂ (41), or in other words 1300 to 2500 Pg carbon. This may however be an overestimate, because the total amount released was most likely greatly reduced by rapid back-reactions (42,43) in which 40-80% of volatilised CaO and CO₂ immediately recombined within the plume to re-form CaCO₃ (30). As for sulphur, we do not include in the model calculations any consequences of lime produced alongside the CO₂.

A global heat-shock (44) following the impact may have ignited woody biomass, leading to wildfires (45), and thence CO₂ release to the atmosphere. In the Late Cretaceous the total biomass of living vegetation was possibly larger than it is today (~600 Pg C), because forests extended closer to the poles at that time (46). Although there are much larger estimates of the amount of vegetation burnt (up to 2700 Pg C,

ref. 47, based on the amount of soot produced and assuming it all came from wildfires), it seems to us unlikely that burning of terrestrial vegetation carbon could have contributed much more than 1500 Pg C, both because of mid-continent aridity in warmer climates (48) and because of finite habitat space.

An additional potential carbon source comes from soils. The throwing up of large amounts of soot, aerosols and dust to the atmosphere probably led to an extended period of darkness on Earth, during which photosynthesis was strongly inhibited by low light levels (49). During this period, decay of soil organic carbon (turnover time today of about 50 years, ref. 50), would not have been balanced by replenishment from new production of leaf litter and other sources associated with living plants. We assumed a maximum total for the Late Cretaceous of 2500 Pg C (compared to 1600 Pg C today), taking into account that soil carbon stocks on Earth today are much higher towards the poles, particularly in permafrost regions. Although the planet was warmer on the whole in the Late Cretaceous, the lack of ice-sheets on Antarctica at that time could have allowed large soil carbon stocks to accumulate there (51).

We modelled the effect on ocean carbonate chemistry from all of these sources combined, through a family of model runs with carbon additions (to the atmosphere rather than the surface ocean) of 2000, 4000 and 6500 Pg C. The sources most likely released carbon both rapidly (volatilisation of carbonate rocks at the point of impact, wildfires) and slowly (decay of soil carbon). We therefore carried out runs in which CO₂ was added to the atmosphere both more slowly (*e*-folding times of between 0.5 and 10 years) and more rapidly (*e*-folding time of 10 hours). Results of these

carbonate rock runs are shown in figures 1, 2 and S1. Large impacts are produced, although not as severe as from the largest sulphuric acid additions. In contrast to the response to SO₄, there is little difference between the responses to CO₂ added with *e*-folding times of 6 months and 10 hours, because of slow air-sea gas exchange of CO₂.

240

241

236

237

238

239

<FIGURE 2 TO GO HERE>

242

243

244

245

246

247

248

249

250

251

252

253

254

255

256

257

258

(3) Nitrogen oxides due to atmospheric shock wave.

As the asteroid (and subsequent ejecta) travelled at high speed through the atmosphere, the associated intense pressure wave would have led to conversion of N₂ and O₂ in the atmosphere to NO_X. Upon conversion to nitric acid (HNO₃) and incorporation into rain, this would have induced acidification of the ocean as it rained out over the following months or years (or possibly days if also scavenged by large silicate particles). Although the total amount of HNO₃ produced directly by the initial pressure wave (~1 x 10¹⁵ mol, ref. 52) is relatively small, it could have been doubled by HNO₃ from ejecta pressure waves (53), and supplemented by ~3 x 10¹⁵ mol HNO₃ from wildfires (47), giving rise to maximum total additions of up to 5 x 10¹⁵ mol HNO₃. Nitric acid addition reduces surface water total alkalinity (TA) in the molar ratio HNO₃:TA = 1:-1 (40). We implemented this hypothesis with a set of runs of different NOx additions (1, 3 and 5 x 10^{15} mol) over a range of e-folding times (0.5, 1, 5 and 10 years). The results are shown in figures 1 and 2 (and figure S1). The impact on ocean carbonate chemistry is similar in nature to that from sulphuric acid, but considerably smaller (5 x 10^{15} mol HNO $_3$ has the same impact on TA as 2.5 x 10^{15} mol H₂SO₄, or in other words less impact than the minimum sulphur run).

260

(4) Breakdown of ocean stratification.

Large tsunamis occurred within 1000 km of Chicxulub (27) and other effects (the shock wave, and secondary tsunamis following impact-induced earthquakes and the return of ejecta) would have led to more widespread consequences for ocean stratification. If the overall disturbance was sufficient to bring about a global mixing between surface and intermediate depth (lower pH) waters, then surface ocean pH would have dropped. This scenario was implemented in model runs by increasing the amount of mixing (initially by a factor (α) of 2, 5, 10 or 100-fold above normal), with the mixing rate (K) over time (t) subsequently decaying back to the baseline value (K') over e-folding timescales (τ) of between 6 months and 10 years, according to the equation:

272
$$K(t) = K' \left[1 + (\alpha - 1) e^{\left(\frac{-t}{\tau}\right)} \right]$$
(3)

274 Results are shown in figures 1 and S1.

(5) Combined scenarios.

Additional runs ($\tau = 6$ months or $\tau = 10$ hours) were carried out in which all acidifying factors were set to their maximum amounts, except for the input of SO_4 from sulphate aerosols which was the only factor varied between runs. The input of nitric acid was thus set to 5 x 10^{15} mol and the input of CO_2 to 6500 Gt C (exceeding an estimate of 4600 Pg C for the total CO_2 input, ref. 23). Changes to ocean stratification were not simultaneously modelled because they weaken the combined impact. The results from these runs are shown in Table 1 and figure 3.

Discussion

Sulphate aerosols were most likely the dominant acidifying factor.
It is clear that some processes have much greater potential than others to drive
extinction-level OA. Considering firstly inputs of CO ₂ (from wildfires, decay, and
release from rocks), it appears that the potential for mass extinction-scale OA impacts
in this case is limited. Even for the largest total amount (6500 Pg C) over the shortest
timescale (10 hours), the model produces a minimum $\Omega_{calcite}$ of 2.2. Such an impact
would not have been sufficiently severe to produce complete global extinction of most
calcifying species via shell dissolution. This maximum amount of 6500 Pg C at the
K/Pg compares to ~600 Pg C of anthropogenic carbon released to date (2015) in the
Anthropocene (1) and estimated total available fossil fuel reserves of about 4000 Pg
C. It can be seen (table 1), however, that the addition of the same amount of carbon to
the modern system would reduce $\Omega_{calcite}$ to a much lower average value (0.7).
Breakdown of ocean stratification is seen to have only a relatively small potential to
lower seawater pH and Ω_{calcite} . This is not surprising, because the pH of intermediate
waters in most oceans is about 7.7 and this sets a limit to the decrease in pH that can
be achieved by a sudden stirring of the oceans. Although very deep waters are
undersaturated with respect to calcium carbonate, this is primarily due to the effect of
pressure. For instance, if water from 3.5 km deep in the North Atlantic (dissolved
inorganic carbon (DIC) = 2180 μ mol kg ⁻¹ , total alkalinity (TA) = 2340 μ mol kg ⁻¹)
were to be raised to the surface and the pressure effect removed, its $\Omega_{calcite}$ would be
~2.8. In the North Pacific, where deep water has accumulated more products of
decomposition, $\Omega_{calcite}$ after removal of the pressure effect would be ~1.8. In neither
case would the water be at all undersaturated ($\Omega_{calcite}$ would not be < 1). Although

long-term sustained changes in mixing can have a great impact over hundreds of thousands of years on the depth of the CCD and the $\delta^{13}C$ of CaCO₃ (54), short term effects on surface ocean $\Omega_{calcite}$ are modest and this mechanism can also be ruled out as a cause of severe OA at the K/Pg.

Of the two processes in which acid is directly added to the surface ocean (sulphuric and nitric acid additions), the former far outweighs the latter in terms of maximum possible OA impacts. The nitric acid additions do not cause severe OA (table 1) even for the highest estimate of the amount added (5 x 10^{15} mol N). Therefore, this too can be discounted as a sole cause of severe OA.

The only process capable by itself of producing severe undersaturation (here defined as Ω -calcite < 0.5; the choice of this threshold is discussed below) is the deposition of sulphuric acid. In fact, even when all other acidifying factors are set to their maximum values and combined, in the absence of sulphate aerosols then the total effect is not sufficient to induce undersaturation (row 7 "All except SO₄" in table 1). In the rest of this paper we thus focus on impacts relating to sulphuric acid additions to the ocean.

How much sulphur was released?

A key uncertainty in the assessment of OA at the K/Pg is therefore the magnitude of sulphur release, which depends on several factors. An important uncertainty is the size of the impactor, with early calculations made for bodies of diameter 10, 15 or 20 km, whereas later calculations were based on smaller sizes such as 10 km, in line with downwards revision of the size of the impactor (27). There is disagreement about the pressure required to vaporise gypsum and release sulphur oxides. Earlier papers such

as that by Sigurdsson et al. (36) assumed that 20 to 40 GPa are required, leading to higher estimates of the amounts vaporised. Later studies (e.g. 31) assumed a requirement of 100 GPa. There is also uncertainty about the angle at which the impactor hit the Earth. It may have been a vertical, full-on impact (angle of incidence = 90°, ref. 56) or alternatively may have hit at a shallower angle (20 to 30°, ref. 27). Additional uncertainty comes from lack of complete knowledge about the nature of the impact site geology and more specifically the amount of gypsum in the impacted rocks. Another source of uncertainty is that most estimates assume that 100% of the volatilised sulphur ends up as sulphuric acid, whereas it has been suggested (30,31) that about 50% was reincorporated almost immediately into solid CaSO₄ as it reformed due to back-reactions within the plume.

These uncertainties lead to a greater than 10-fold range in the predictions of sulphuric acid delivered to the surface ocean, as discussed earlier, which translates into considerable uncertainty about OA impacts. Additional model runs (figures 3 and S4; table S1) show that the critical amount of SO₄ needed to reduce Ω -calcite to a value of 0.5 is between 8 and 43 x 10^{15} mol, depending on the rapidity of addition and on the intensity of other acidifying processes. Between 30 and 43 x 10^{15} mol is required if SO₄ is added relatively slowly ($\tau = 6$ months), whereas between 8 and 10 x 10^{15} mol is required if SO₄ need to be compared to estimates of how much sulphur was actually released, up to 60 x 10^{15} mol according to the studies used by D'Hondt et al. (25), or between 0.9 and 9 x 10^{15} mol according to the most recent analysis (31). Our model runs therefore suggest that Ω_{calcite} could have fallen below the threshold of 0.5 for many of the SO₄ emissions used by D'Hondt et al (25), but only for the upper end of the range

proposed by the most recent study (31). The very high estimate used by D'Hondt et al. (25) came from only one of the three studies they cited, which was 5- to 20-fold higher than the maximum estimate from the other two studies cited and nearly an order of magnitude higher than the top end of the range from the most recent analysis (table 2). The difference has been ascribed (56) primarily to Sigurdsson et al's assumption that gypsum vaporisation can occur at lower pressures.

Could OA at the K/Pg have been severe enough to cause calcifier extinctions?

In order to answer this question, it is necessary to estimate a lower limit value of Ω below which calcifiers could not have survived. Despite large amounts of ongoing research into the impacts of OA on the marine biota, a precise value for such a Ω threshold is not yet available, and in any case differs between calcifier species (57). We use a critical threshold value of Ω_{calcite} of 0.5 in the surface ocean. This criterion of $\Omega_{\text{calcite}} < 0.5$ corresponds to those waters becoming strongly undersaturated for calcite, the less soluble form of CaCO3 accreted by coccolithophores (calcareous nannoplankton) and foraminifera to form shells. Because high latitudes and low latitudes are not distinguished in this simple model, there is only one surface box and hence only one value of Ω_{calcite} . In nature, on the other hand, there is a latitudinal gradient in Ω in surface waters, with highest values (at low latitudes) on average about 20% higher than the global average (58). A global average value of $\Omega_{\text{calcite}} = 0.5$ therefore corresponds to surface oceans being quite strongly undersaturated for both calcite and aragonite at all latitudes. However, some calcifying species continue to calcify quite well (in the laboratory at least) even at $\Omega_{\text{calcite}} = 0.5$ (e.g. refs. 57 and 59).

This threshold should therefore be considered as the minimum degree of corrosivity to CaCO₃ that is required to account for widespread calcifer extinctions, and it is possible that even lower average values would actually be required. As discussed above, the only scenarios making surface seawater so corrosive are those in which large amounts of sulphur are released rapidly from gypsum rocks.

390

391

392

393

394

395

396

397

398

399

400

401

402

403

404

405

406

407

408

409

385

386

387

388

389

Overall, our model results do not point to extremely severe OA at the K/Pg, although they do not completely rule it out. We conclude that it is possible but not likely that the numerous calcifier extinctions were due to OA. Some reasons for this conclusion are as follows: (A) out of several factors considered in the simulated scenarios, only one (sulphuric acid) made the surface ocean strongly corrosive to calcite (Ω_{calcite} < 0.5); (B) even for sulphuric acid, the amount required to produce severe OA (previous section, table S1) is above the upper ends of most (including the most recent) estimates of ranges of possible emissions (table 2); (C) the amounts of H₂SO₄ reaching the surface ocean were probably at least 2-fold less than the early estimates of the amounts of S released, because they ignored rapid back-reactions consuming sulphur in the plume (30); and (D) the release of S to the atmosphere may have been accompanied by a production of lime (CaO) (30) and/or other basic compounds (39), which if subsequently falling into the surface ocean may have dissolved there, raising Ω_{calcite} and pH. Other explanations for selective extinctions should therefore continue to be explored, such as the suggestion (60) that groups with resting stages (e.g. dinoflagellates cysts or diatom spores) were able to survive better than those without (including calcareous nannoplankton). Further progress on this question would be assisted by a better understanding of both the magnitude and rapidity of sulphuric acid additions.

Although a preliminary inspection of the K/Pg paleontological record strongly supports an OA-driven calcifier extinction, when considered in greater detail the evidence appears less compelling. For instance, in contrast to calcareous nannoplankton, another group of calcifying plankton, the calcareous dinoflagellates, experienced no major extinction at the K/Pg (18). All calcareous rudist bivalve species were lost (61), but out of bivalves as a whole ~35% of 'sub-genera' survived (62). In contrast to planktics, benthic foraminifera with calcareous shells survived the event relatively intact, whether inhabiting shallow or deep waters (63). Inoceramid clams underwent 100% extinction but up to 13% of bryozoans and only rather few marine gastropods went extinct (16).

Zooxanthellate scleractinian corals (those which host photosynthetic algal symbionts, and which are therefore restricted to living in shallow waters where peak OA impacts would have been greatest) suffered much greater species extinction rates than azooxanthellate scleractinian corals inhabiting a much larger depth range (64). In fact deep water corals, far from being preferentially killed off, instead preferentially survived the end-Cretaceous mass extinction (64). This is compatible with much more severe OA in surface than in deeper waters, as is seen in our models (plots not shown). However, among scleractinian corals as a whole (zooxanthellate and azooxanthellate combined) only ~50% of all species were lost, which would seem surprising if OA was the cause for other calcifier extinctions, given the experimental and field evidence showing coral sensitivity to OA (65). According to Kiessling & Simpson (66): "During the major mass extinctions at the end of the Ordovician,

Permian and Cretaceous periods [the calcifying groups] corals and coralline sponges have indistinguishable extinction rates from other taxa."

436

437

438

439

440

441

442

443

444

445

446

447

448

449

450

451

452

434

435

Comparison to previous calculations

Some of these acidifying processes were considered in earlier work by D'Hondt et al. (25). Although D'Hondt et al calculated the effects of adding acids to the ocean without the aid of a dynamical model such as that used here, their earlier predictions are broadly consistent with our model results. We have considered a much wider range of possible acidifying processes, but concur that the process of gypsum vaporisation is likely to be quantitatively the most important. Our estimate of the amount of sulphur required to explain extinctions, in the absence of other processes, is however much less: 43 x 10¹⁵ mol SO₄ (or 10 x 10¹⁵ mol SO₄ if added very rapidly, but see table S1 for sensitivity of these numbers to assumptions) compared to their estimate of 61 x 10¹⁵ mol SO₄. In agreement with Ohno et al. (21), our model results show lower $\Omega_{calcite}$ values when SO₄ is added more rapidly than when it is added more slowly. However, contrary to their calculations, in our model we find that 1 x 10¹⁴ kg H_2SO_4 ($\approx 1 \times 10^{15}$ mol SO_4) is not nearly enough to produce strong undersaturation (panel B of figure S4). Our model results therefore support an earlier assessment (53) that nitric acid could only have caused minor acidification and that sulphuric acid was unlikely to have led to significant acidification.

454

453

455

Conclusions

457

Results have been presented from our carbon cycle modelling study of ocean acidification (OA) at the end of the Cretaceous. The effects of several acidifying mechanisms were simulated, including wildfires emitting CO2 to the atmosphere and vaporisation of gypsum rocks leading to deposition of sulphuric acid on the ocean surface. Our assessment of the potential for OA from these mechanisms finds that most produce too small an impact on the CaCO₃ saturation of the surface ocean to be able to explain the simultaneous extinctions of calcifiers. Only sulphuric acid deposition is capable of making the surface oceans strongly corrosive to calcite. However, in order to produce severe CaCO₃ undersaturation ($\Omega_{\text{calcite}} < 0.5$), very large quantities (greater than between 8 and 43 x 10¹⁵ moles, depending on assumptions about the rate of addition and the intensities of other acidifying processes) of sulphur must have been volatilised from gypsum and anhydrite in sedimentary rocks. 8 x 10¹⁵ moles is right at the top of recent estimates (0.8 to 8 x 10¹⁵ moles). Hence we think it rather unlikely, although not completely impossible, that biologically catastrophic OA occurred at the Cretaceous-Paleogene (K/Pg) boundary. The great extinctions of calcifiers at this time (100% of ammonites and rudist bivalves, more than 90% of calcareous nannoplankton and planktic foraminifera species) were most likely due to some other cause.

476

475

458

459

460

461

462

463

464

465

466

467

468

469

470

471

472

473

474

477

478

479

480

481

Methods summary

The global biogeochemical box model.

The main biogeochemical box model (JModel) used here is a variant of one used previously to study a number of different carbon cycle and OA problems (54, 67-69).

The model (for more details see supplementary information) represents the coupled global ocean and atmosphere. It includes phytoplankton, phosphorus, dissolved inorganic carbon (DIC) and alkalinity as state variables. The model fully resolves the carbonate system; ocean carbon chemistry is linked, through air-sea gas exchange, with atmospheric CO₂. Although long-term feedbacks are not relevant for this study, the model includes a dynamic calcite compensation depth (CCD).

Simulations.

We started the model in steady state with geochemical conditions appropriate for the late Cretaceous (66 Myr ago). The atmospheric CO_2 concentration was 1,000 ppmv, the calcium ion concentration was 20 mmol kg^{-1} (e.g. ref. 7) and the magnesium ion concentration was 30 mmol kg^{-1} (pre-industrial values are 280 ppmv, 10.3 mmol kg^{-1} and 53 mmol kg^{-1} respectively). The effects of altered $[Ca^{2+}]$ and $[Mg^{2+}]$ on K_1 , K_2 (the carbonate system equilibrium constants) and K_{sp} (the $CaCO_3$ solubility product) were calculated following ref. 70, with additional runs (see table S1) to investigate sensitivity to alternative values of atmospheric CO_2 and K_{sp} . The starting state of the model was obtained by holding the atmospheric CO_2 fixed at its target value (1000 ppmv) before running the model out to equilibrium. For each hypothesis we carried out a set of model runs with different magnitudes and timescales of perturbation. The rate of addition (R) over time (t) of a total amount (t) of a substance was calculated from the t-folding timescale (t) according to:

$$R(t) = \frac{A}{\tau} e^{\left(\frac{-t}{\tau}\right)} \tag{1}$$

In order to assess the robustness of the results obtained, we carried out sensitivity analyses (to different surface layer depths, K_{sp} values, and initial atmospheric CO_2 value; table S1) and repeated the tests in different model setups: (1) the same model (JModel) as just described, but in its pre-industrial configuration, i.e. with atmospheric CO_2 and seawater Ca and Mg concentrations set to Holocene levels rather than adjusted to resemble the Late Cretaceous ocean (results shown in table 1 and figures S2 and S3); and (2) the independent LOSCAR model, which is a box model with more boxes than the JModel and with explicit sediments (71). LOSCAR was configured to resemble the late Paleocene ocean. Results of these alternative model setups are shown in table 1.

Acknowledgements

We gratefully acknowledge insightful discussions with Andy Ridgwell, Ken Caldeira, Eric Achterberg, Jay Melosh, and Dani Schmidt. We thank Richard Zeebe for assistance with use of his LOSCAR model. This work was a contribution to the European Project on Ocean Acidification (EPOCA), which received funding from the European Community's Seventh Framework Programme (FP7/2007-2013) under grant agreement no. 211384.

526 **References**

- 527 1. Raupach MR & Canadell JG (2010) Carbon and the Anthropocene. *Curr Opin* 528 Sust 2(4):210-218.
- 529 2. Sabine CL & Tanhua T (2010) Estimation of Anthropogenic CO2 Inventories in the Ocean. *Annu Rev Mar Sci* 2:175-198.
- 531 3. Gattuso J-P & Hansson L (2011) *Ocean acidification* (Oxford University Press, Oxford; New York) pp xix, 326 p.
- 533 4. Riebesell U, Fabry VJ, Hansson L, & Gattuso J-P eds (2010) *Guide to best*534 practices for ocean acidification research and data reporting (Publications
 535 Office of the European Union, Luxembourg), p 260.
- 536 5. Collins S & Bell G (2004) Phenotypic consequences of 1,000 generations of selection at elevated CO2 in a green alga. *Nature* 431(7008):566-569.
- 538 6. Lohbeck KT, Riebesell U, & Reusch TBH (2012) Adaptive evolution of a key phytoplankton species to ocean acidification. *Nat Geosci* 5(5):346-351.
- Honisch B, et al. (2012) The Geological Record of Ocean Acidification.
 Science 335(6072):1058-1063.
- Zeebe RE & Westbroek P (2003) A simple model for the CaCO3 saturation
 state of the ocean: The "Strangelove," the "Neritan," and the "Cretan" Ocean. *Geochemistry, Geophysics, Geosystems*, 4(12), 1104,
 doi:10.1029/2003GC000538.
- Zeebe RE (2012) History of seawater carbonate chemistry, atmospheric CO2,
 and ocean acidification. *Annual Review of Earth and Planetary Sciences* 40:141-165.
- 549 10. Ridgwell A & Schmidt DN (2010) Past constraints on the vulnerability of marine calcifiers to massive carbon dioxide release. *Nat Geosci* 3(3):196-200.
- 551 11. Caldeira K & Wickett ME (2003) Anthropogenic carbon and ocean pH. 552 *Nature* 425(6956):365-365.
- Renne PR, *et al.* (2013) Time Scales of Critical Events Around the Cretaceous-Paleogene Boundary. *Science* 339(6120):684-687.
- 555 13. Marshall CR & Ward PD (1996) Sudden and gradual molluscan extinctions in the latest Cretaceous of western European Tethys. *Science* 274(5291):1360-557 1363.
- Bown P (2005) Selective calcareous nannoplankton survivorship at the Cretaceous-Tertiary boundary. *Geology* 33(8):653-656.
- Jiang SJ, Bralower TJ, Patzkowsky ME, Kump LR, & Schueth JD (2010)
 Geographic controls on nannoplankton extinction across the
 Cretaceous/Palaeogene boundary. *Nat Geosci* 3(4):280-285.
- 563 16. Macleod N, *et al.* (1997) The Cretaceous-Tertiary biotic transition. *Journal of the Geological Society* 154:265-292.
- Racki G (1999) Silica-secreting biota and mass extinctions: survival patterns and processes. *Palaeogeogr Palaeocl* 154(1-2):107-132.
- Wendler J & Willems H (2002) Distribution pattern of calcareous
 dinoflagellate cysts across the Cretaceous-Tertiary boundary (Fish Clay,
 Stevns Klint, Denmark): Implications for our understanding of species-
- 570 selective extinction. *Catastrophic Events and Mass Extinctions: Impacts and*
- 571 Beyond, eds Koeberel C & MacLeod KG (Geological Society of America
- 572 Special Paper 356), pp 265-275.

- 573 19. Medlin LK, Saez AG, & Young JR (2008) A molecular clock for
- 574 coccolithophores and implications for selectivity of phytoplankton extinctions 575 across the K/T boundary. *Marine Micropaleontology* 67(1-2):69-86.
- 576 20. Alegret L, Thomas E, & Lohmann KC (2012) End-Cretaceous marine mass extinction not caused by productivity collapse. *P Natl Acad Sci USA* 109(3):728-732.
- 579 21. Ohno S, *et al.* (2014) Production of sulphate-rich vapour during the Chicxulub impact and implications for ocean acidification. *Nat Geosci* 7(4):279-282.
- Caldeira K & Rampino MR (1993) Aftermath of the End-Cretaceous Mass
 Extinction Possible Biogeochemical Stabilization of the Carbon-Cycle and
 Climate. *Paleoceanography* 8(4):515-525.
- 584 23. Beerling DJ, Lomax BH, Royer DL, Upchurch GR, & Kump LR (2002) An 585 atmospheric pCO(2) reconstruction across the Cretaceous-Tertiary boundary 586 from leaf megafossils. *P Natl Acad Sci USA* 99(12):7836-7840.
- 587 24. Huang C, Retallack GJ, Wang C & Huang Q (2013) Paleoatmospheric pCO₂
 588 fluctuations across the Cretaceous–Tertiary boundary recorded from paleosol
 589 carbonates in NE China. *Palaeogeography*, *Palaeoclimatology*,
 590 *Palaeoecology* 385:95-105.
- 591 25. D'Hondt S, Pilson MEQ, Sigurdsson H, Hanson AK, & Carey S (1994)
 592 Surface-Water Acidification and Extinction at the Cretaceous-Tertiary
 593 Boundary. *Geology* 22(11):983-986.
- 594 26. Smit J (1999) The global stratigraphy of the Cretaceous-Tertiary boundary 595 impact ejecta. *Annual Review of Earth and Planetary Sciences* 27:75-113.
- 596 27. Schulte P, *et al.* (2010) The Chicxulub Asteroid Impact and Mass Extinction at the Cretaceous-Paleogene Boundary. *Science* 327(5970):1214-1218.
- 598 28. Kring DA (2007) The Chicxulub impact event and its environmental consequences at the Cretaceous-Tertiary boundary. *Palaeogeogr Palaeocl* 255(1-2):4-21.
- Gerasimov MV, Dikov YP, Yakovlev OI, & Wlotzka F (1994) High temperature vaporization of gypsum and anhydrites: experimental results. In
 Lunar and Planetary Institute Science Conference Abstracts (Vol. 25, p. 413).
 Lunar and Planetary Institute Science Conference Abstracts, p 413.
- Agrinier P, Deutsch A, Schärer U & Martinez I (2001) Fast back-reactions of
 shock-released CO₂ from carbonates: an experimental approach. *Geochimica et Cosmochimica Acta* 65(15):2615-2632.
- 608 31. Pierazzo E, Hahmann AN, & Sloan LC (2003) Chicxulub and climate: 609 Radiative perturbations of impact-produced S-bearing gases. *Astrobiology* 610 3(1):99-118.
- Thornton DC, Bandy AR, Blomquist BW, Driedger AR, & Wade TP (1999)
 Sulfur dioxide distribution over the Pacific Ocean 1991-1996. J Geophys Res Atmos 104(D5):5845-5854.
- 614 33. Oppenheimer C, Scaillet B & Martin RS (2011) Sulfur degassing from volcanoes: source conditions, surveillance, plume chemistry and Earth System impacts. *Reviews in Mineralogy and Geochemistry* 73(1):363-421.
- Barnes JE & Hofmann DJ (1997) Lidar measurements of stratospheric aerosol over Mauna Loa Observatory. *Geophys Res Lett* 24(15):1923-1926.
- 619 35. Pope KO, Baines KH, Ocampo AC & Ivanov BA (1994) Impact winter and the Cretaceous/Tertiary extinctions: results of a Chicxulub asteroid impact model. *Earth and Planetary Science Letters* 128(3):719-725.

- Sigurdsson H, Dhondt S, & Carey S (1992) The Impact of the Cretaceous
 Tertiary Bolide on Evaporite Terrane and Generation of Major Sulfuric-Acid
 Aerosol. Earth Planet Sc Lett 109(3-4):543-559.
- Brett R (1992) The Cretaceous-Tertiary Extinction a Lethal Mechanism
 Involving Anhydrite Target Rocks. *Geochim Cosmochim Ac* 56(9):3603-3606.
- 38. Pope KO, Ocampo AC, Baines KH & Ivanov BA (1993) Global blackout
 following the K/T Chicxulub impact: Results of impact and atmospheric
 modeling. In Lunar and Planetary Institute Science Conference Abstracts (Vol.
 24, p. 1165). Lunar and Planetary Science Conference Abstracts, p 1165.
- 631 39. Maruoka T & Koeberl C (2003) Acid-neutralizing scenario after the Cretaceous-Tertiary impact event. *Geology* 31(6):489-492.
- 633 40. Doney SC, *et al.* (2007) Impact of anthropogenic atmospheric nitrogen and sulfur deposition on ocean acidification and the inorganic carbon system. *P Natl Acad Sci USA* 104(37):14580-14585.
- 636 41. O'Keefe JD & Ahrens TJ (1989) Impact production of CO₂ by the Cretaceous 637 Tertiary extinction bolide and the resultant heating of the Earth. *Nature* 638 338(6212):247-249.
- Ivanov BA & Deutsch A (2002) The phase diagram of CaCO₃ in relation to shock compression and decomposition. *Physics of the Earth and Planetary Interiors* 129(1-2):131-143.
- 43. Yancey TE & Guillemette RN (2008) Carbonate accretionary lapilli in distal
 deposits of the Chicxulub impact event. *Geological Society of America* Bulletin 120(9-10):1105-1118.
- 645 44. Goldin TJ & Melosh HJ (2009) Self-shielding of thermal radiation by Chicxulub impact ejecta: Firestorm or fizzle? *Geology* 37(12):1135-1138.
- 647 45. Morgan J, Artemieva N, & Goldin T (2013) Revisiting wildfires at the K-Pg boundary. *J Geophys Res-Biogeo* 118(4):1508-1520.
- 649 46. Spicer RA (2003) Changing climate and biota. *The Cretaceous World*, ed Skelton PW (Cambridge University Press, Cambridge), pp 85-162.
- 651 47. Crutzen PJ (1987) Mass extinctions acid-rain at the K/T Boundary. *Nature* 652 330(6144):108-109.
- 653 48. Skelton PW (2003) *The Cretaceous world* (Open University : Cambridge University Press, Cambridge, U.K.; New York) p 360 p.
- Vellekoop J, Sluijs A, Smit J, Schouten S, Weijers JWH, Sinninghe Damsté
 JS, & Brinkhuis H (2014) Rapid short-term cooling following the Chicxulub
 impact at the Cretaceous–Paleogene boundary. *Proc. Natl Acad Sci USA* 111(21): 7537-7541.
- 659 50. Giardina CP & Ryan MG (2000) Evidence that decomposition rates of organic 660 carbon in mineral soil do not vary with temperature. *Nature* 404(6780):858-661 861.
- DeConto RM, Galeotti S, Pagani M, Tracy D, Schaefer K, Zhang T, Pollard R
 & Beerling DJ (2012) Past extreme warming events linked to massive carbon release from thawing permafrost. *Nature* 484(7392):87-91.
- 52. Zahnle KJ (1990) Atmospheric chemistry by large impacts. *Geological Society* of America Special Papers, 247:271-288.
- Toon OB, Zahnle K, Morrison D, Turco RP, & Covey C (1997)
 Environmental perturbations caused by the impacts of asteroids and comets.
- 669 *Rev Geophys* 35(1):41-78.

- 670 54. Merico A, Tyrrell T, & Wilson PA (2008) Eocene/oligocene ocean de-671 acidification linked to Antarctic glaciation by sea-level fall. *Nature* 672 452(7190):979-U976.
- 673 55. Pierazzo E, Kring DA, & Melosh HJ (1998) Hydrocode simulation of the Chicxulub impact event and the production of climatically active gases. *J Geophys Res-Planet* 103(E12):28607-28625.
- 676 56. Kring DA & Durda DD (2002) Trajectories and distribution of material ejected from the Chicxulub impact crater: Implications for postimpact wildfires. *J Geophys Res-Planet* 107(E8).
- 679 57. Ries JB, Cohen AL, & McCorkle DC (2009) Marine calcifiers exhibit mixed responses to CO2-induced ocean acidification. *Geology* 37(12):1131-1134.
- 681 58. Orr JC, *et al.* (2005) Anthropogenic ocean acidification over the twenty-first century and its impact on calcifying organisms. *Nature* 437(7059):681-686.
- Trimborn S, Langer G, & Rost B (2007) Effect of varying calcium
 concentrations and light intensities on calcification and photosynthesis in
 Emiliania huxleyi. *Limnol Oceanogr* 52(5):2285-2293.
- 686 60. Ribeiro S, *et al.* (2011) Phytoplankton growth after a century of dormancy illuminates past resilience to catastrophic darkness. *Nat Commun* 2.
- 688 61. Steuber T, Mitchell SF, Buhl D, Gunter G, & Kasper HU (2002) Catastrophic extinction of Caribbean rudist bivalves at the Cretaceous-Tertiary boundary. *Geology* 30(11):999-1002.
- 691 62. Lockwood R (2003) Abundance not linked to survival across the end-692 cretaceous mass extinction: Patterns in North American bivalves. *P Natl Acad* 693 *Sci USA* 100(5):2478-2482.
- 694 63. Culver SJ (2003) Benthic foraminifera across the Cretaceous—Tertiary (K–T) boundary: a review. *Marine Micropaleontology* 47:177-226.
- 696 64. Kiessling W & Baron-Szabo RC (2004) Extinction and recovery patterns of scleractinian corals at the Cretaceous-Tertiary boundary. *Palaeogeogr Palaeocl* 214(3):195-223.
- 699 65. Hoegh-Guldberg O, *et al.* (2007) Coral reefs under rapid climate change and ocean acidification. *Science* 318(5857):1737-1742.
- 701 66. Kiessling W & Simpson C (2011) On the potential for ocean acidification to be a general cause of ancient reef crises. *Global Change Biol* 17(1):56-67.
- 703 67. Chuck A, Tyrrell T, Totterdell IJ, & Holligan PM (2005) The oceanic response to carbon emissions over the next century: investigation using three ocean carbon cycle models. *Tellus B* 57(1):70-86.
- 706 68. Tyrrell T, Shepherd JG, & Castle S (2007) The long-term legacy of fossil fuels. *Tellus B* 59(4):664-672.
- 708 69. Bernie D, Lowe J, Tyrrell T, & Legge O (2010) Influence of mitigation policy on ocean acidification. *Geophys Res Lett* 37.
- 710 70. Tyrrell T & Zeebe RE (2004) History of carbonate ion concentration over the last 100 million years. *Geochim Cosmochim Ac* 68: 3521-3530.
- 712 71. Zeebe RE (2012) LOSCAR: Long-term Ocean-atmosphere-Sediment CArbon
 713 cycle Reservoir Model v2.0.4. *Geosci Model Dev* 5(1):149-166.

714 **Table 1:** Severity of impacts in different models.

	Alkalinity removal	moval Carbon Minimum surface $\Omega_{ m calcite}^*$			2 _{calcite} *	Duration
	from surf. ocean	from surf. ocean addition to			of peak	
		atm.				impact [‡]
			JModel	LOSCAR [†]	JModel	
Scenario	(PMol)	(Pg)	(Cretaceous)	(Paleocene)	(Pre-industrial)	
Gypsum vaporisation (SO ₄)	120	-	<u>0.0</u>	0.0	<u>0.0</u>	<5 y
NO _x generation	5	-	6.1	3.6	3.8	<5 y
Carbon dioxide (CO ₂)	-	6500	2.2	1.4	0.7	ky
Stirring	-	-	5.4	-	3.8	<5 y
All	125	6500	<u>0.0</u>	0.0	0.0	<5 y
All except SO ₄	5	6500	2.1	1.0	0.6	<5 y
Rapid addition of SO ₄	120	-	<u>0.0</u>	0.0	-	<1 y
Rapid addition of NO _x	5	-	3.4	-	-	<1 y
Rapid addition of CO ₂	-	6500	2.2			

^{*} For each scenario the lowest minimum Ω_{calcite} is taken from the run in which the largest amount of substance (for instance 60×10^{15} Mol, for

SO₄) is added over an e-folding time of 6 months, except for rapid additions where the e-folding time was 10 hours. Initial values of surface

^{717 \}Quad \Omega_{calcite} \text{ were 7.5 (JModel-Cretaceous), 4.9 (LOSCAR-Paleocene, ref. 71) and 4.9 (JModel-pre-industrial)

^{718 &}lt;sup>†</sup> Average across all ocean basins. A run with increased stirring was not implemented for this model.

[‡] Time for which Ω_{calcite} was at least 80% as far from the initial value as when at its maximum distance.

Table 2: Estimates of sulphur release associated with the impact.

	Estimated sulphur input to the atmosphere			
Source	PMol (= 10 ¹⁵ mol) S	Pg S		
Sigurdsson et al., 1992	0.2 to 132	6 to 4200		
Brett, 1992	6	200		
Pope et al., 1993	8 to 26	270 to 820		
Chen et al., 1994	1 to 9	32 to 290		
Ivanov et al., 1996	1 to 3	32 to 96		
Pierazzo et al., 1998	2 to 17	54 to 560		
Maruoka & Koeberl,	2 to 11	78 to 364		
2003				
Pierazzo et al., 2003	0.9 to 9	30 to 300		

Figure Captions

724

725

726

727

728

729

730

731

732

733

734

735

736

737

738

739

740

741

742

Figure 1: Impacts of different scenarios of environmental change on surface ocean chemistry: (top row) pH; (bottom row) saturation state for calcite (Ω_{calcite}). Each column shows the acidification impacts for a different type of forcing (same vertical axis scale for each) when the forcing is applied with an e-folding time of 6 months. Minimum $\Omega_{calcite}$ values for each model run are shown in the boxes. The colour of each line indicates the magnitude of the forcing for that run. **Figure 2:** Impacts of very rapid additions (*e*-folding time of 10 hours, ref. 21) of H₂SO₄ (column 1), CO₂ (column 2), and HNO₃ (column 3) on saturation state for calcite. Minimum Ω_{calcite} values for each model run are shown in the boxes. The colour of each line indicates the magnitude of the forcing for that run. **Figure 3:** Impacts on Ω_{calcite} of different quantities of sulphate aerosols acting in combination with maximum quantities of other processes (5 PMol NOx and 6500 Pg C in the form of CO_2). Left column shows results for additions using an e-folding time of 6 months; right column shows results for additions using an e-folding time of 10 hours (21). Minimum Ω_{calcite} values for each model run are shown in square brackets in the boxes. The colour of each line indicates the magnitude of the forcing for that run.

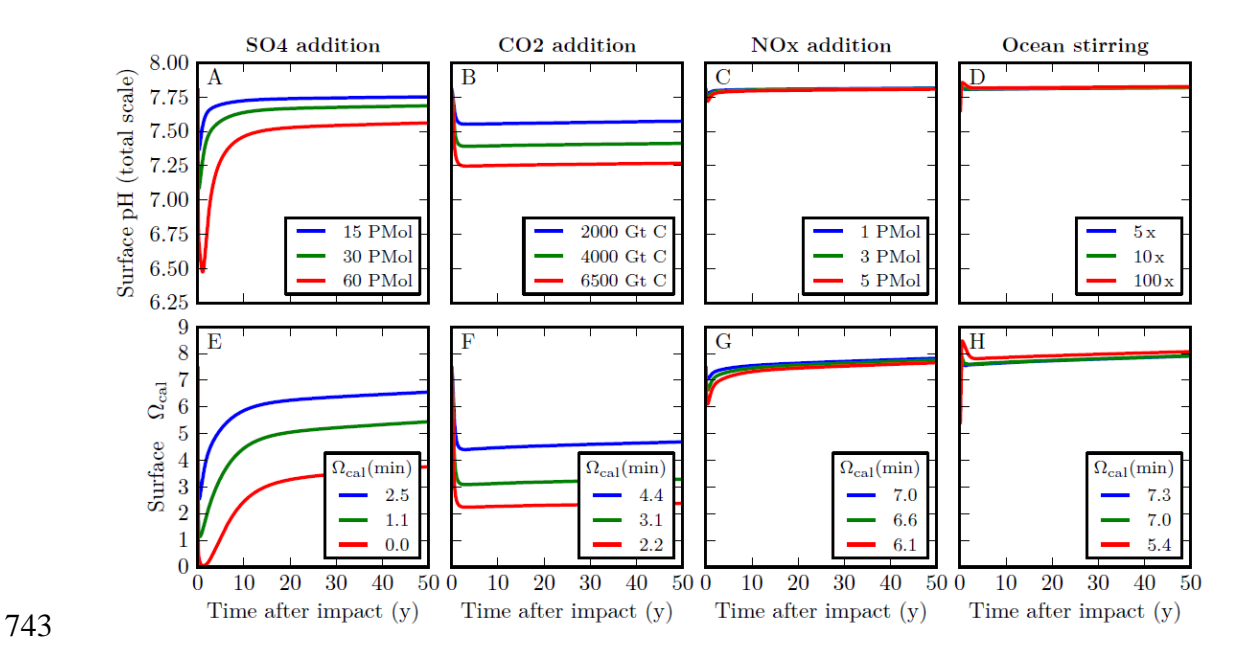


Figure 1: Impacts of different scenarios of environmental change on surface ocean chemistry: (top row) pH; (bottom row) saturation state for calcite ($\Omega_{calcite}$). Each column shows the acidification impacts for a different type of forcing (same vertical axis scale for each) when the forcing is applied with an e-folding time of 6 months. Minimum $\Omega_{calcite}$ values for each model run are shown in the boxes. The colour of each line indicates the magnitude of the forcing for that run.

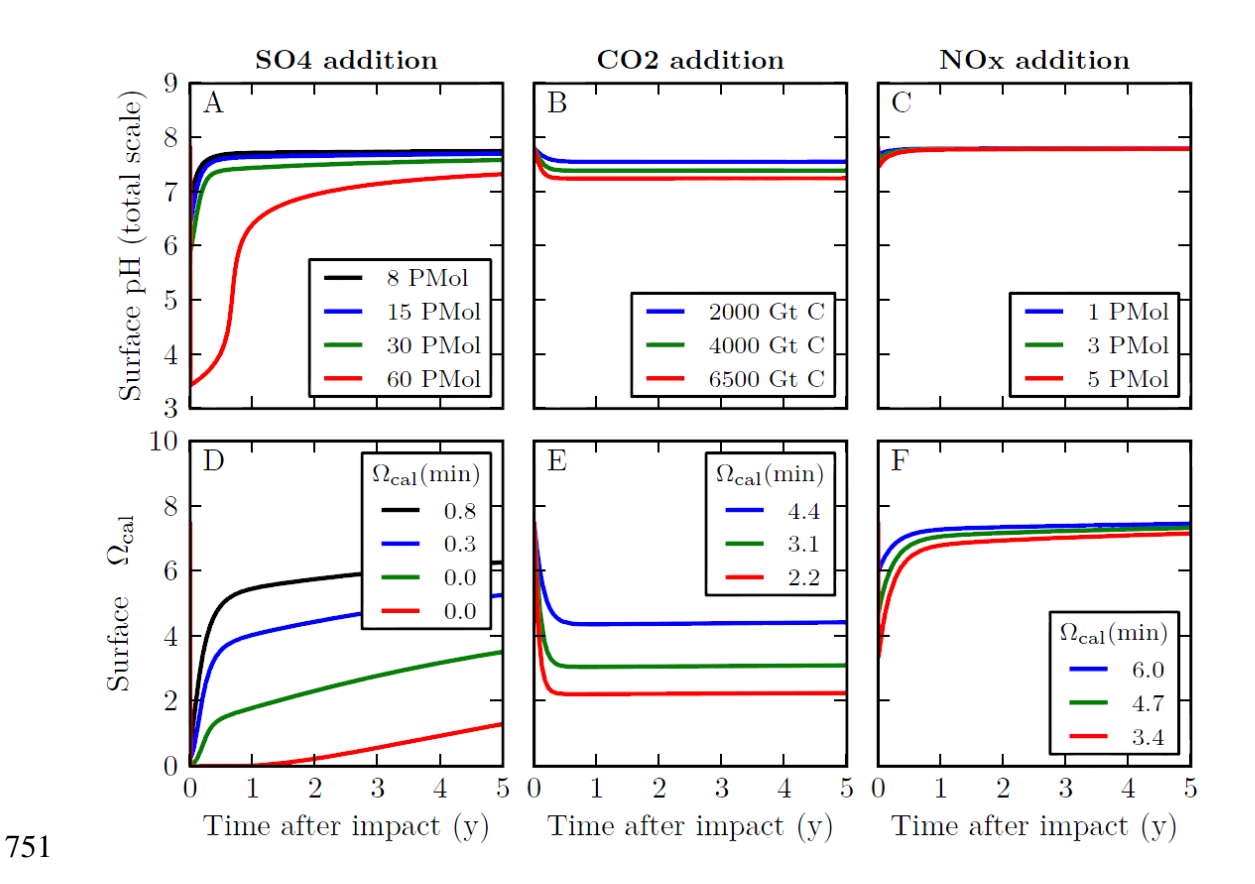


Figure 2: Impacts of very rapid additions (e-folding time of 10 hours, ref. 21) of H_2SO_4 (column 1), CO_2 (column 2), and HNO_3 (column 3) on saturation state for calcite. Minimum $\Omega_{calcite}$ values for each model run are shown in the boxes. The colour of each line indicates the magnitude of the forcing for that run.

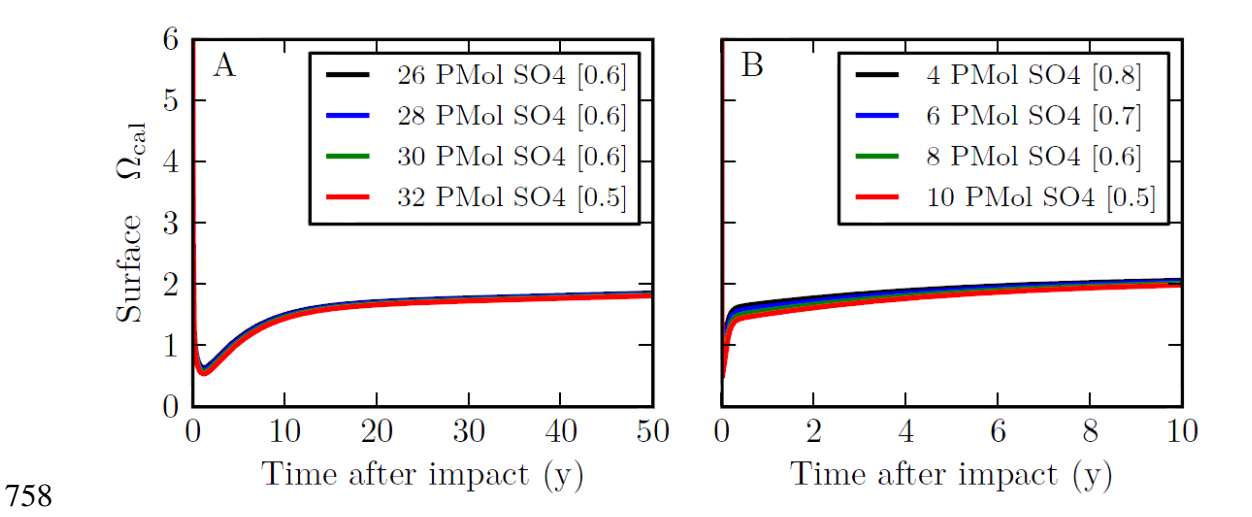


Figure 3: Impacts on $\Omega_{calcite}$ of different quantities of sulphate aerosols acting in combination with maximum quantities of other processes (5 PMol NOx and 6500 Pg C in the form of CO₂). Panel A shows results for additions using an e-folding time of 6 months; Panel B shows results for additions using an e-folding time of 10 hours (21). Minimum $\Omega_{calcite}$ values for each model run are shown in square brackets in the boxes. The colour of each line indicates the magnitude of the forcing for that run.

Supplementary Information

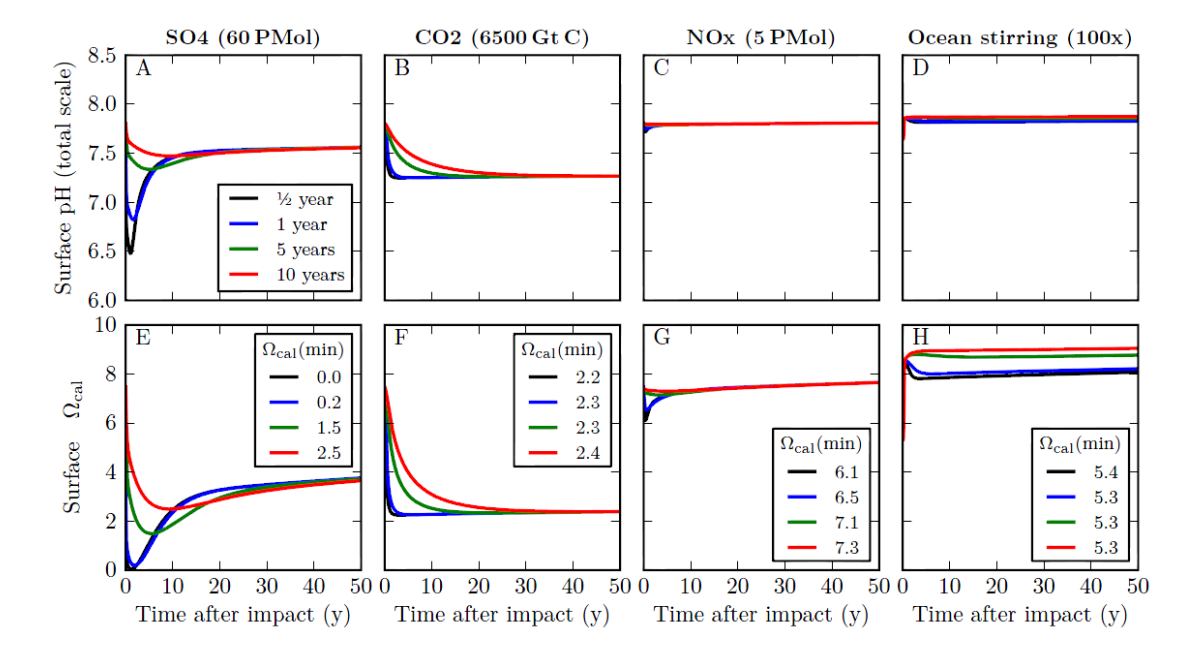


Figure S1: Impacts of different scenarios of environmental change on surface ocean chemistry: (top row) pH; (bottom row) saturation state for calcite (Ω_{calcite}). Each column shows the acidification impacts for a different type of forcing (same vertical axis scale for each) with the magnitude of the forcing shown at the top of the column. The colour of each line indicates the rapidity (e-folding time) of the forcing.

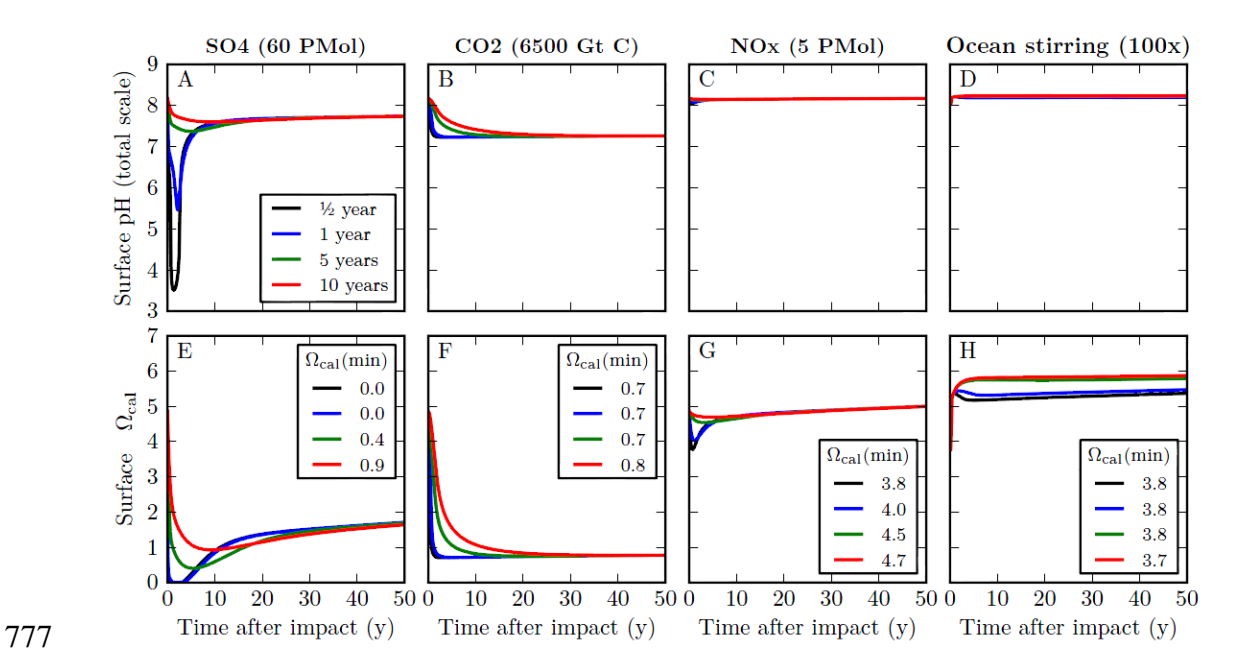


Figure S2: Impacts of different scenarios of environmental change on surface ocean chemistry in the pre-industrial model setup: (top) pH; and (bottom) Ω_{calcite} . Each column shows the acidification impacts for a different type of forcing (same vertical axis scale for each) with the magnitude of the forcing shown at the top of the column. Minimum Ω_{calcite} values for each run are shown in the box. The colour of each line indicates the rapidity (*e*-folding time) of the forcing.

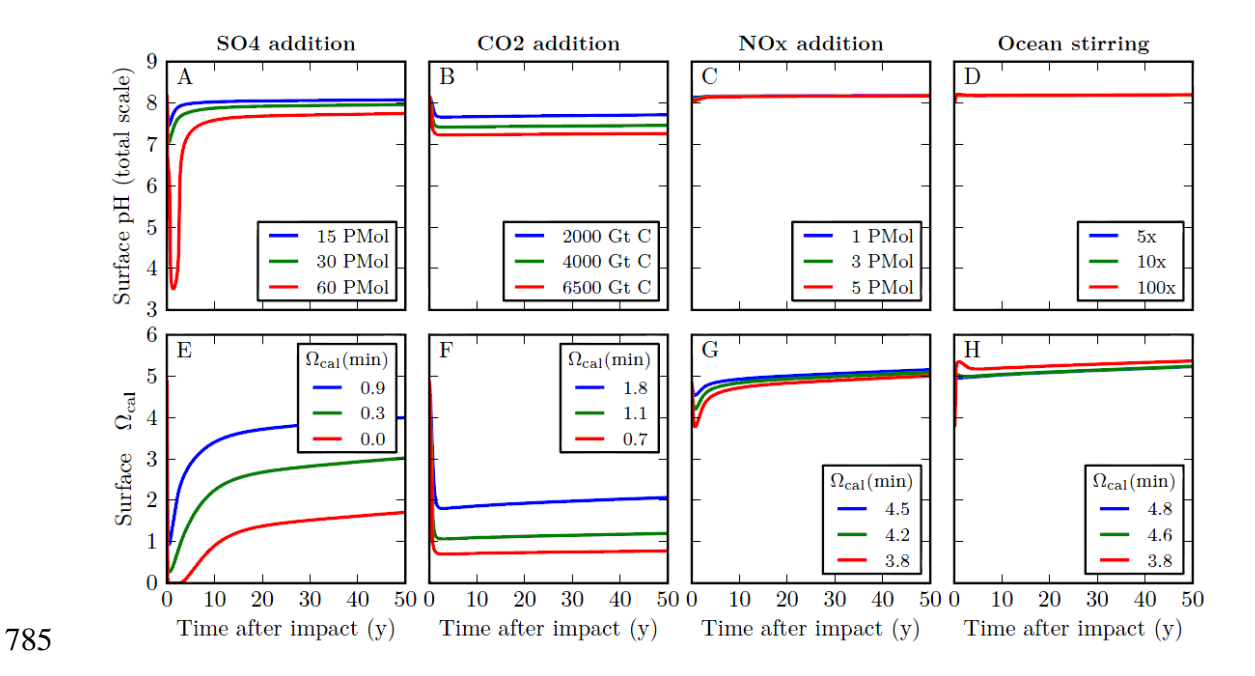


Figure S3: Impacts of different scenarios of environmental change on surface ocean chemistry in the pre-industrial model setup: (top) pH; and (bottom) Ω_{calcite} . Each column shows the acidification impacts for a different type of forcing (same vertical axis scale for each) when the forcing is applied using an e-folding timescale of 6 months. The colour of each line indicates the magnitude of the forcing.

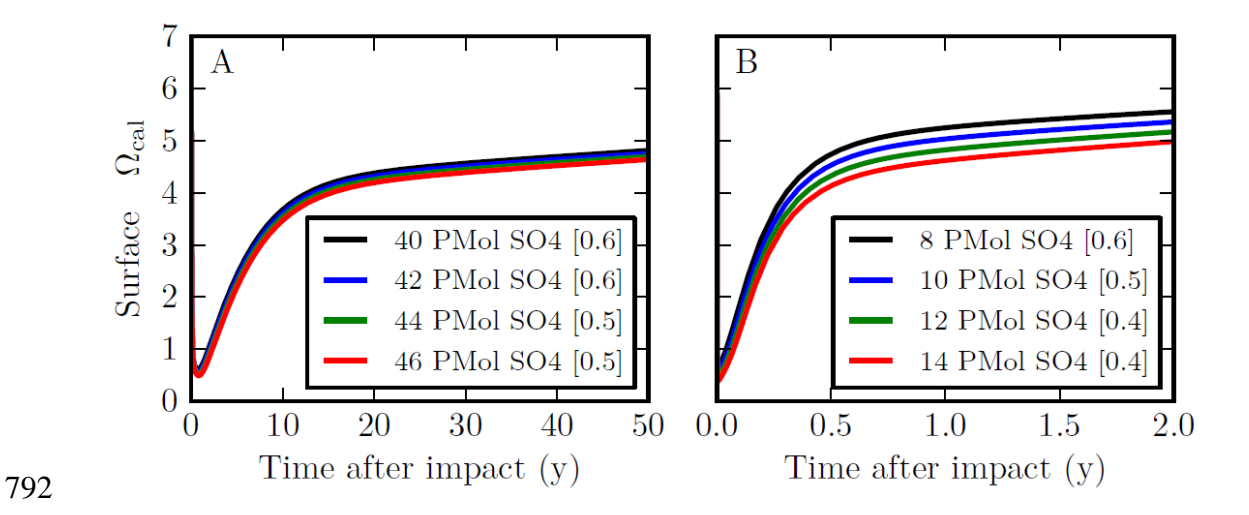


Figure S4: Impacts on Ω_{calcite} of different quantities of sulphate aerosols acting alone (all other processes omitted) on saturation state for calcite in the surface box. Panel A shows results for additions using an e-folding time of 6 months; Panel B shows results for additions using an e-folding time of 10 hours (20). This plot shows similar results to those for SO4 in figures 1 and 2, but here the effects of a much narrower range of sulphur emissions are plotted, to show the amount required to cause severe $CaCO_3$ undersaturation (Ω -calcite < 0.5). Minimum Ω_{calcite} values for each model run are shown in square brackets in the boxes. The colour of each line indicates the magnitude of the forcing for that run.

Table S1: Results of sensitivity analyses calculating the sensitivity of the critical amount of SO_4 to some key model assumptions. Default values are K_{spc} (end Cretaceous) / K_{spc} (modern) = 0.7, a surface mixed layer depth of 100 m, and an initial (spin-up) atmospheric CO_2 concentration of 1000 ppm.

		Amount of SO ₄ (PMol S) required to produce Ω -calcite < 0.5					
		<i>e</i> -folding time of 6 months		<i>e</i> -folding time of 10 hours			
		acting alone	acting in	acting	acting in		
Sensitivity Analysis			combination	alone	combination		
standard run (for comparison)		43	30	10	8		
ratio of K _{spc} (end Cret)	0.8	44	30	11	8		
to	0.9	45	31	11	8		
$K_{spc}(modern)$	1.0	45	31	11	8		
mixed layer depth (m)	75	35	23	8	6		
	50	26	17	6	3		
	30	18	11	4	1		
initial atm CO ₂ (ppm)	500	31	17	8	6		
	2000	55	43	14	12		
No primary production (biological		43	30	11	8		
pump) after the impact							

Methods details

As illustrated in figure S5, the model ocean is structured as three vertically stacked boxes: the surface (0-100 m) which represents the euphotic zone, a middle box (100-500 m) which represents the mixed surface layer above the annual thermocline, and a deep box (500-3730 m) representing the deep layer below the annual thermocline. The assumed depth of the surface box is an important parameter for this study because it determines the volume of water into which acidifying substances are initially diluted. We used the same mixed layer depth as D'Hondt et al. (23), i.e. 100 m. The surface mixed layer is shallower than 100 m across most of the ocean and so we also carried out sensitivity analyses (table S1) for alternative choices of 50 m and 30 m, although we note that any process causing global extinctions has to exterminate species across all of their ranges, including where deeper mixed layer depths prevail. The model represents an average water column down to the seabed, has a spatially and temporally averaged input of nutrients, DIC (dissolved inorganic carbon) and alkalinity, and does not take into account any latitudinal or horizontal variations.

The rate of growth of phytoplankton is a function of their intrinsic maximum growth rate and modulation by nutrient (in this case phosphate) scarcity according to a Michaelis-Menten relationship. After being produced, phytoplankton biomass either decays within the surface ocean box (returning nutrient and carbon back to solution) or else, following export, decays within a lower box, or else is lost to the system through permanent burial. There is only one variable for phytoplankton; separate types are not distinguished in the model. Calcification is calculated in a fixed ratio to new organic matter (see below) and the resulting CaCO₃ is then either dissolved in the deep ocean

following export or else is buried, with the relative proportions calculated according to a complex relationship between the carbonate saturation of the deep ocean (determining the depth of the CCD) and the average hypsometry of the seafloor.

837

838

839

840

841

842

843

844

845

846

847

848

849

850

851

852

853

854

834

835

836

As in other models, carbonate chemistry is modeled by including DIC and alkalinity as state variables. The distribution of DIC within the ocean is governed by physical, chemical and biological processes: the exchange of CO₂ between the atmosphere and the ocean, riverine input of DIC, biological uptake of carbon into phytoplankton biomass, remineralisation and burial of that biomass, precipitation and dissolution of CaCO₃, and mixing processes between the three layers. The distribution of alkalinity in the ocean is governed by riverine input of bicarbonate, precipitation of CaCO₃ by calcifying organisms, dissolution of CaCO₃ deeper in the ocean, burial of CaCO₃ and mixing processes between the three layers. As and when necessary, other carbonate system parameters are calculated from DIC and alkalinity with the program csys (68) using the constants of Mehrbach et al (69) as refit by Lueker et al. (70). These constants are unlikely to be realistic under the most extreme conditions modelled here; however, this deficiency is likely to be most serious at Ω -calcite below 0.5, and so will not affect our ability to detect whether such a state occurs. Since the model uses phosphorus as the only limiting nutrient, the impact of riverine nitrate input, biological uptake of nitrate, and remineralisation of nitrate on alkalinity is accounted for via the Redfield ratio.

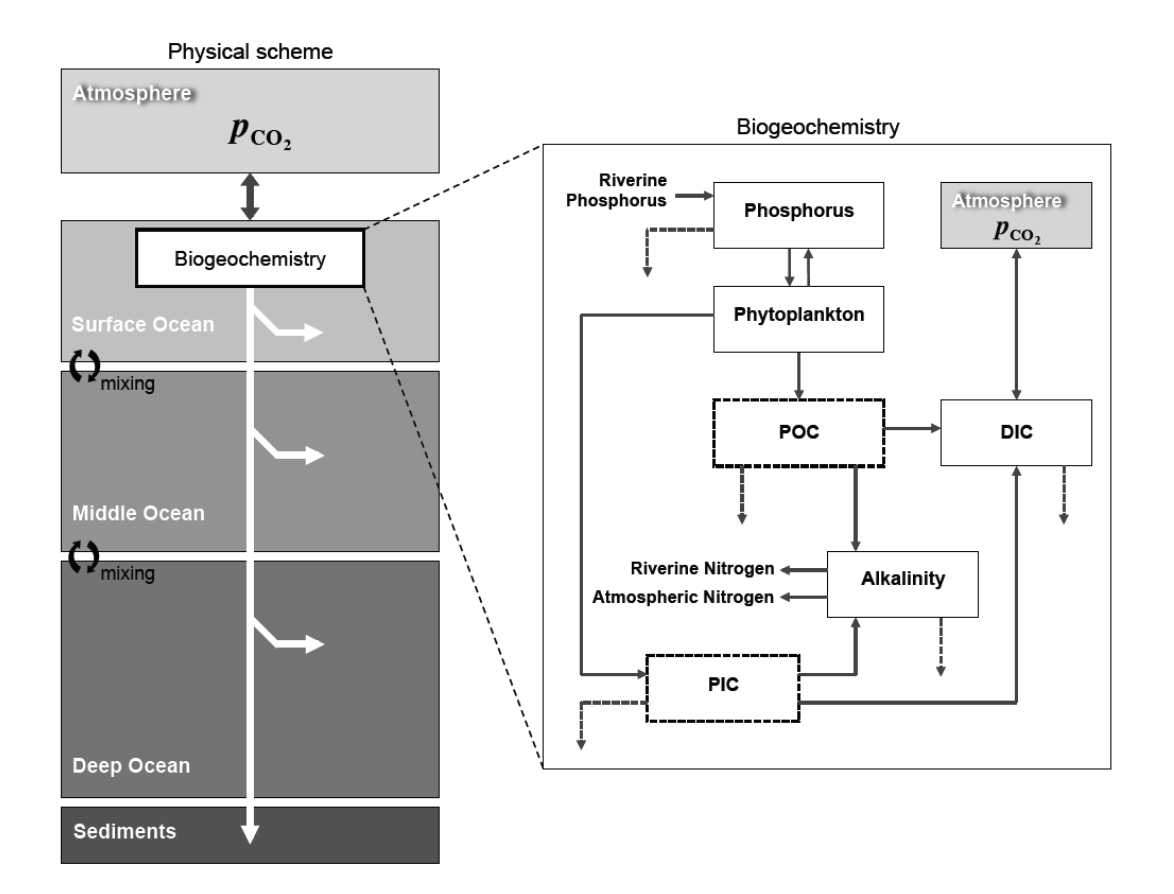


Figure S5: Schematic of the model. A three-box ocean (surface box thickness = 100m, middle box thickness = 400m, deep box thickness = 3230m) and an atmosphere exchange carbon dioxide, with implicit carbon loss to the sediment layer. In the biogeochemistry scheme, the dashed black arrows represent export from the surface ocean. PIC indicates particulate inorganic carbon while POC indicates particulate organic carbon. The arrows in the oceanic boxes and sediments represent the various remineralization and sedimentation fluxes.

The production of CaCO₃ in the surface ocean is linked to the production of organic matter through the "rain ratio" (RR), which is the molar ratio of CaCO₃-C export from the surface layer to particulate organic carbon (POC) export. The influence of sediments on the cycling of carbon is not considered in our model and is not important in this study because we focus only on short-term impacts (up to a few centuries).

- 871 68. Zeebe RE & Wolf-Gladrow DA (2001) *CO₂ in seawater : equilibrium, kinetics, isotopes* (Elsevier, Amsterdam ; New York) pp xiii, 346 p.
- 873 69. Mehrbach C, Culberson CH, Hawley JE, & Pytkowicz RM (1973) 874 Measurement of the apparent dissociation constant of carbonic acid in 875 seawater at atmospheric pressure. *Limnol Oceanogr* 18:897-907.

Lueker TJ, Dickson AG, & Keeling CD (2000) Ocean pCO(2) calculated from dissolved inorganic carbon, alkalinity, and equations for K-1 and K-2: validation based on laboratory measurements of CO2 in gas and seawater at equilibrium. *Mar Chem* 70(1-3):105-119.